*SF2A 2007*
*J. Bouvier, A. Chalabaev, C. Charbonnel (eds)*

# THE ACCRETION-EJECTION INSTABILITY AND MICROQUASARS

P. Varnière[1], M. Tagger[2], J. Rodriguez[3] and M. Cadolle Bel[4]

**Abstract.** We will shortly review the Accretion-Ejection Instability and show how to provides a good model to explain the Low-Frequency QPO from microquasars. From that we will show how the Magnetic Flood Scenario can explain the variability class $\beta$ of GRS 1915+105 and how to extend it beyond that class.

## 1 Introduction

Microquasars are low-mass X-ray binaries which exhibit powerful ultra-relativistic jets (see e.g. the review of Mirabel & Rodriguez, 1999) and are thought to host a black hole. Microquasars are observed in different spectral states: the high state where the disk thermal emission is dominant, the low state where a non-thermal power-law dominates the thermal emission, and an intermediate state where both are seen.

In the low state, and sometimes in the intermediate state, we observe low frequency (of the order of 1 to 30 Hertz) Quasi-Periodic Oscillations (LFQPO) of the X-ray flux (e.g. Fender, 2001). The right panel of figure **??** shows the low-frequency QPO of GRS 1915+105.

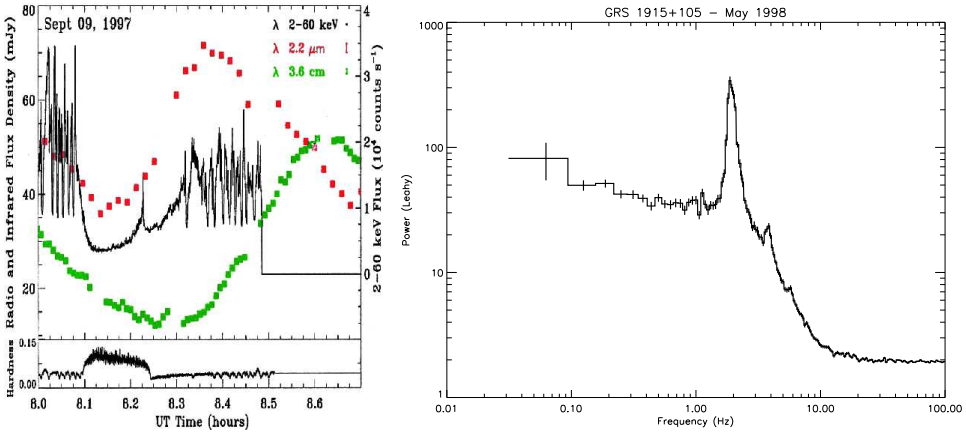


**Fig. 1.** The left figure is a multi-wavelength observation of GRS 1915+105 with X-ray data in black, and infra-red in red, radio in green (Mirabel *et al.*, 1998). It is the class $\beta$ of Belloni *et al.* (1999) with the LFQPO observed in the low state (before the X-ray peak) and with ejection occurring at the X-ray peak. The right figure represents a Fourier transform of the X-ray light curve for the same object (G. Markwardt). The LFQPO is prominent at a frequency of two Hertz, and higher harmonics are also seen.

These low-frequency QPOs seem to be associated with radio emission, usually interpreted to imply the presence of a jet. The left figure shows multi-wavelength observations of the same object during an ultra-relativistic ejection. The black curve (X-ray data) shows a transition from the high state (without LFQPO)

[1] LAOG, Universit J. Fourier (UMR5571), France
[2] Service d'Astrophysique (UMR APC), CEA Saclay, 91191 Gif-sur-Yvette, France
[3] Service d'Astrophysique (UMR AIM), CEA Saclay, 91191 Gif-sur-Yvette, France;
[4] ESA/ESAC, Villafranca del Castillo, Madrid, Spain

to the low state (with LFQPO) and a return to the high state (without LFQPO). The disappearance of the LFQPO is concurrent with the X-ray spike, which also seems to be concurrent with emission of the plasmoid observed in the infra-red and radio (red and green points).

In addition to the low frequency (1-30Hz) QPOs, high frequency QPOs are observed in neutron star binaries ($\sim kHz$) and sometimes also in black hole systems ($\sim 70-450$, Hz depending on mass). Here we focus on the low frequency QPOs, which unlike the high frequency QPOs, are *ubiquitous in black hole systems*, see e.g. the review by Remillard & McClintock (2006) and review how the Accretion-Ejection Instability might be at the origin of it.

## 2 The Accretion-Ejection Instability

### *2.1 The Basics*

The AEI is a spiral instability, similar to galactic spiral density waves but driven by magnetic stresses rather than self-gravity (Tagger & Pellat, 1999). It occurs in the inner region of an accretion disk threaded by a vertical magnetic field when the latter is of the order of equipartition with the gas pressure, i.e. a plasma $\beta = 8\pi p/B^2 \sim 1$. This magnetic configuration is also the one used as an initial condition in almost all MHD jet models (for e.g. Blandford Payne 1982, Pelletier & Pudritz, 1992). Because of the strong magnetic field required, this instability develops in a region where the Magneto-Rotational Instability (MRI, Balbus & Hawley, 1991) has likely shut down. The origin of such a strong magnetic field may come from an in situ large scale helical dynamo (e.g. Blackman & Field 2002) or be accreted from the exterior with the flow. Regardless of the origin of such a field, its plausibility is supported by observations of our Galactic center where strong vertical magnetic filaments with $\beta \sim 1$ are observed. (e.g. Chandran, Cowley & Morris 2000).

The AEI creates a 1-armed spiral pattern rotating in the disk at a frequency of the order of a few tenths of $\Omega_{int}$ (i.e. 1/10 the rotation frequency at the inner edge of the disk). The spiral grows by extracting energy and angular momentum from the inner region of the disk, and stores them in a Rossby vortex generated at its corotation radius. This exchange of energy and angular momentum makes the whole perturbation (density wave + Rossby wave) unstable. With this instability, accretion energy and angular momentum are transported by waves and do not heat up the disk, except by spiral shocks.

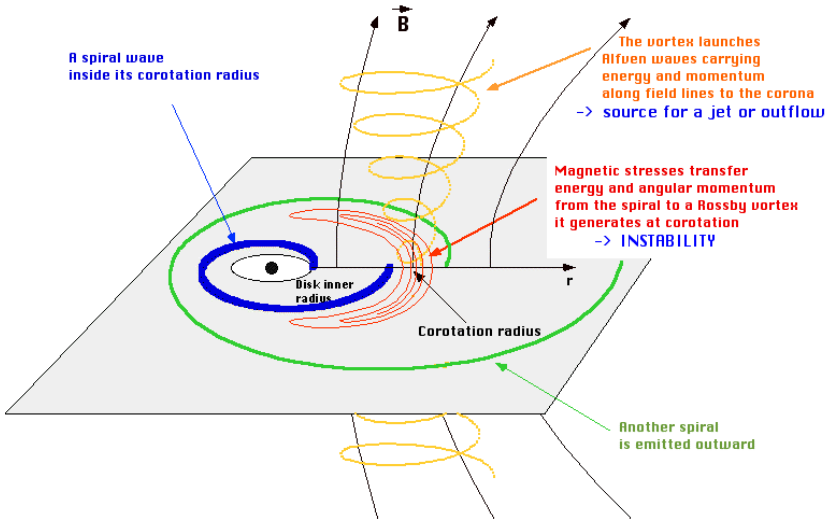


**Fig. 2.** The structure of the instability is shown schematically. It is formed of a standing spiral density wave in the inner part of the disk coupled to a Rossby vortex it excites at itscorotation radius. The Rossby vortex generates Alfvén waves propagating toward the corona of the disk.

Figure **??** illustrates the instability mechanism. A standing wave pattern forms, similar to spiral waves in galaxies. The spiral wave propagates outward from the inner radius of the disk until it is reflected at corotation. In this process the Rossby wave becomes a standing vortex, rotating at the angular velocity of the pattern.

This basic physical description was obtained from the simple model of a thin disk in vacuum, and numerical solutions were given in TP99. If one takes into account a low density corona above the disk, the vortex then leaks energy and angular momentum as Alfvén waves to the corona, where it might power a wind or a jet. The computation of the associated Alfvén wave emission was done in Varnière and Tagger, 2002, which revelealed that a large amount of the accretion energy is sent toward the corona as Alfvén waves. The AEI thus appears to be a good candidate to connect accretion and energy ejection in the inner region of a magnetized disk.

### *2.2 A Modulation of the disk Emission*

A 2D verification of the non-linear evolution of the AEI was done by Caunt & Tagger (2001). The code, although based on a Zeus-type grid, is similar to that used for galactic spirals. It uses cylindrical coordinates with a radial logarimthic grid This allows high precision in the inner part of disk where he instability is developing, and a large dynamic range in $r$ (typically 50 inner radii). The grid also avoids the need to impose a reflective outer boundary. The code also implements the FARGO scheme (Masset, 2000) which enhances execution speed by eliminating the Keplerian speed from the Courant condition. As a last characteristic the disk is assumed to be in the vacuum which allows us to compute the magnetic field through a Poisson equation similar to the self-gravity case in galaxies.

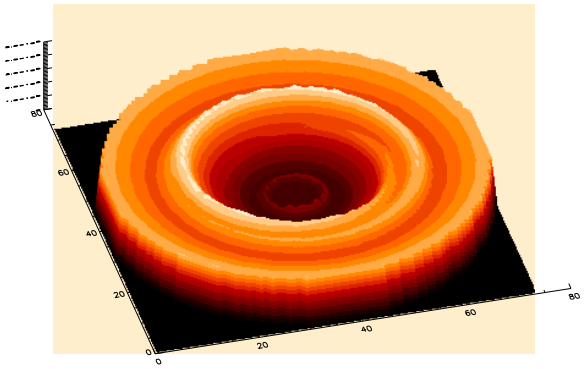


We have upgraded the code by adding an energy equation and computing the local disk thickness using hydrostatic equilibrium. This provides the 3D view of the disk seen on the left. Working with M.Muno at MIT we computed the flux received from such a source and obtained a modulation with significant features comparable to that seen in the observed LFQPOs. However the rms amplitude of the simulated light curve is only 5% while the observed one sometimes reaches 20%.

The source of the rms modulation in the AEI model results from a combination of two effects: 1) the anisotropy associated with the disk due to the presence of spiral waves 2) the disk inclination angle, and 3) the height of the hot spiral. This difference in rms amplitude between the 2-D AEI and the observations very likely comes from the fact that the height of the spiral wave is not simulated but computed a posteriori. To improve this situation requires 3-D simulations, which in turn will allow much more realistic synthetic spectra of microquasars to be produced. The 2-D simulations have at least demonstrated the possibility of obtaining such modulations.

### *2.3 Alfven Waves Emission Toward the Corona*

The AEI can send energy toward the corona from the Rossby vortex. Indeed, the vortex twists the footpoints of field lines threading the disk, generating Alfvén waves propagating to the corona (see **??**). In Varnière & Tagger 2002, we present a detailed calculation of this mechanism.

The amplification of the wave (and thus the flux deposited by the spiral in the vortex) and the flux transmitted to Alfvén waves are both linked to the singular nature of the vortex. This allows us to give in a very simple form an estimate of the fraction of the accretion energy, extracted from the inner region of the disk, which will end up in the corona where it might feed a jet. This fraction is of the order of unity if the coronal density is not too low (typically $10^{-4}$ of the density in the disk would be sufficient, in an X-ray binary).

## 3 The AEI and Observations

### *3.1 The Low-Frequency QPO*

The significance of the LFQPOs can be summarized as follows (Remillard & McClintock 2006):

(1) LFQPOs are always present during the Low Hard state, but are also almost always seen during the "steep power-law state", which is the non-thermal state that accreting black holes exhibit when they reach their highest luminosities (i.e. $L_X > 0.4\ L_{Edd}$). They can be exceedingly strong with rms amplitudes (expressed as a fraction of the mean count rate) as high as $r > 0.15$ for sources such as GRS 1915+105 (Morgan et al. 1997) and XTE J1550–564 (Sobczak et al. 2000). More generally, they are seen with $0.03 < r < 0.15$ whenever the steep power law contributes more than 20% of the flux at 2–20 keV (Sobczak et al. 2000). LFQPOs have been observed up to energies above 60 keV (Tomsick et al. 2001).

(2) In several sources, the LFQPO frequency is correlated with the total disk flux (but not with temperature or inner disk radius; Sobczak et al. 2000; Muno et al. 1999; Trudolyubov et al. 1999). This behavior, in combination with the the role of the steep power law mentioned above, suggests that LFQPOs may provide a vital clue on the coupling between the thermal and steep power-law components.

(3) In the case of GRS 1915+105, LFQPOs always appear while the source exhibits a quasi-steady radio jet, which has been imaged (VLBI) on several occasions (Dhawan et al. 2000). Steady radio jets are associated with the "low-hard" state of black hole binaries, where the X-ray spectrum appears as a power-law with a photon index ($\Gamma \sim 1.7$) that is flatter than the steep power-law state ($\Gamma > 2.4$).

(4) LFQPOs can be quasi–stable features that persist for days or weeks. In GRS 1915+105, QPOs at 2.0–4.5 Hz persisted for 6 months during late 1996 and early 1997 (Muno et al. 2001).

(5) In a general sense, it can be argued that oscillations as distinct as these QPOs (often with $Q > 10$), represent global requirements for an organized emitting region. For example, in the context of models in which thermal radiation originates from MHD instabilities, one cannot accept the common picture of numerous and independent magnetic cells, which are distributed throughout the inner disk, unless they are also combined with some large scale coherent structures.

### *3.2 The AEI as a Model for the LFQPO*

The AEI seems to be a promising candidate to explain low-frequency QPOs because it is able to account for the following observational characteristics:

- The LFQPO frequency is $\sim$ few 1/10 the Keplerian frequency at the inner edge of the disk. This is similar to the rotation frequency of the one-armed spiral predicted in the the linear AEI theory and confirmed by the non-linear simulations.
- The AEI can naturally predict not only the frequency of the LFQPO but can also reproduce, partially, the X-ray flux modulation from the variation in disk properties at the location of the spiral wave.
- The AEI does not require external excitation but grows naturally when the $\beta \sim 1$ (the ratio of thermal to magnetic pressure).
- The AEI creates a large scale wave similar to Galactic spiral density waves. The non-linear simulations show that the rotating pattern remains nearly steady, and thus is a able to account for *persistent* LFQPOs.
- The AEI transfers energy and angular momentum toward the corona by Alfvén Waves, thus providing a supply of Poynting flux that may produce the compact jet, often observed in the low-hard state.
- Including general relativity through the existence of a last stable orbit and orbital velocity profile has allowed us to show that the AEI can explain the observed turnover in the correlation between the color radius (= inner disk radius, as determined by the spectral fits) and the LFQPO frequency. (Rodriguez et al 2002; Varnière et al 2002)

  By incorporating the general relativistic effect of a last stable orbit in the AEI calculations, the correlation between the frequency of the spiral wave and the inner edge of the disk is reversed as the disk inner edge approaches the last stable orbit. The figure to the right (Varnière *et al*, 2002) shows the comparison

between the theoretical curve predicted by the AEI near the last stable orbit of the black hole and observational data from the microquasars GRO J1655-40 during its outburst and GRS 1915+105 during two successive 30min cycles.

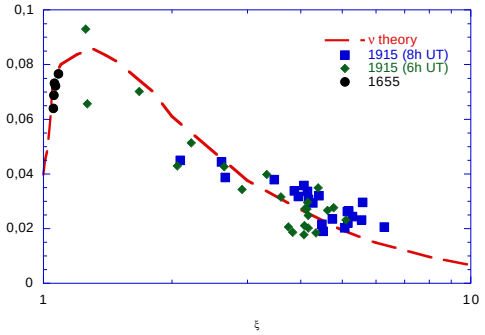


Because of these promising features, we are motivated to further study the AEI as a LFQPO model and compare the predictions to observations.

### *3.3 The Magnetic Flood Scenario*

In 2002, Tagger et al., elaborated on the possible identification of the AEI with the QPO to produce a Magnetic Flood Scenario (MFS) that would explain the characteristic 30 mn cycle ($\beta$ class of Belloni *et al.*, 2001 ) of GRS 1915+105 (fig. below) The MFS explains the repetitive X-ray behavior using a limit cycle determined by the advection of poloidal magnetic flux to the inner disk and its destruction via magnetic reconnection with the magnetic flux trapped close to the source (which can lead to relativistic ejection).

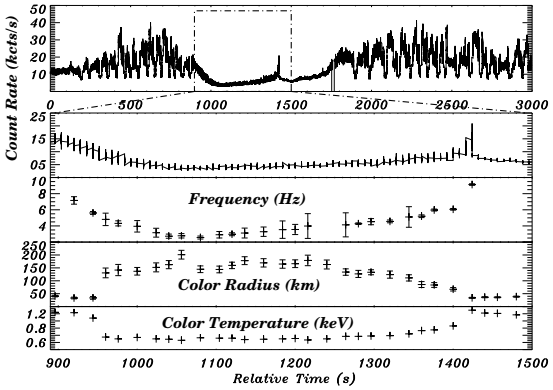


At the beginning of the $\beta$ class the source is the high state, accretion is caused by the Magneto-Rotational Instability (similar to an $\alpha$ prescriprion) which requires a low magnetic field. The vertical magnetic flux builds up in the disk and the $\beta$ decreases slowly, until it reaches $\beta \sim 1$. At that point the MRI stops and the AEI starts. This has two consequences, the temperature decreases with the stopping of turbulent heating, further decreasing the $\beta$ and the LFQPO appears (just before the transition, as it has been observed once). This can explain the abrupt transition observed between the high and low state.

During the low state, the AEI is at the origin of the LFQPO and sends energy toward the corona by the means of Alfven wave. The next striking feature in the $\beta$ class is the intermediate spike. At that instant the LFQPO stops, the coronal emission decreases sharply. and an infra-red synchrotron emission, presumably from a blob ejected at relativistic speed, begins. This ejection (possibly caused by reconnection with the magnetic flux surrounding the black hole) will cause a reorganization of the magnetic field. This causes the disk to return to a higher $\beta$ state, where the MRI can develop again, restarting a new cycle.

The MFS also leads to a natural explanation of the three basic states (A,B and C) from which all the classes of GRS 1915+105 are derived. In the MFS, state C is dominated by the AEI in the inner region of the disk; state A is a soft state where the inner disk is weakly magnetized, after magnetic flux has been destroyed by the reconnection event associated with the relativistic ejection that ends state C. State B is the steep-power law state where magnetic flux has again started piling up near the inner disk edge. The MFS also provides a natural explanation for the observation that the transition from state C to B is never observed: the disk needs to spend some time in state A in order to rebuild enough magnetic flux in its inner region to transition to state B.

## 4 A Unified Model for {Disk + jet }

Fender, Belloni and Gallo (2005) made an important step toward a unified model for the microquasar disk+jet states by producing the evolutionary track shown on the hardness-intensity diagram (shown on the figure **??**) for a variety of black hole binaries. Indeed, objects that appear wildly different in their day-to-day behavior are on similar tracks in the hardness-intensity diagram. An extended version of the MFS has been proposed to

**Fig. 3.** The Hardness-Intensity Diagram of Fender, Belloni and Gallo surimposed with the extended version of the MFS showing the direction of the magnetic flux in the disk and the inner hole.

explain this behavior. It is based on the stored magnetic flux as shown on figure **??**.

If we assume the starting configuration (**1** on the figure) where the magnetic flux stored around the black hole and the disk flux are parallel, the disk innner radius is large and accretion remains weak. Now let us assume a field reversal (dynamo in the disk or the companion) in the flux advected in the disk (**2**), we obtain a slow decrease of the stored flux by (**3**) and at the same time the inner radius of the disk decreases. During all that time, the AEI is present in the disk, it is the low-hard state. At that point there are two possibilities: no field reversal occurs until all the stored flux is cancelled by the disk flux (**4**), we obtain a global reconfiguation of the magnetic field, which favor an ejection and the disk is back at its last stable orbit, or there is a field reversal before that and we obtain a failed-flare as seen sometimes. Slowly the stored flux is rebuilt, parallel to the disk one (**5**), up to a strong stored flux (**6**) which is the same as configuration (**1**) but in the opposite direction.

## 5 Acknowledgments

We would like to thanks the GDR PCHE and the MIT-France program.

## 6 The bibliography

### References

Balbus,S.A. & Hawley,J.F., 1991, ApJ, **376**, 214 & 223

Belloni, T, Klein-Wolt, M.; Méndez, M.; van der Klis, M.; van Paradijs, J., 2000, A&A, **355** 271.

Blackman, E. G. & Field, G. B. 2002, Physical Review Letters, 89, 265007

Blandford, R.D. & Payne, D.G., 1982, MNRAS, **199**, 883.

Caunt, S., Tagger, M., 2001, A&A, 367, 1095,

Chandran, B. D. G., Cowley, S. C., & Morris, M. 2000, ApJ, 528, 723

Dhawan, V., Mirabel, I. F., and Rodriguez, L. F., 2000,ApJ 543, 373.

Fender, R. P., 2001, MNRAS 322, 31-42.

Masset, F., 2000, A&A , 141, 165-173.

Mirabel, I.F.; Dhawan, V; Chaty, S; Rodriguez, L.F.; Marti, J.; Robinson, C.R.; 1998, A& A. Lett., 330 9

Mirabel, I.F. & Rodriguez, L.F., 1999, ARA&A 37, 409.

Muno, Michael P.; Morgan, Edward H.; Remillard, Ronald A., 1999, ApJ, 527, 321.

Muno, Michael P.; Remillard, Ronald A.; Morgan, Edward H.; Waltman, Elizabeth B.; Dhawan, Vivek; Hjellming, Robert M.; Pooley, Guy, 2001, ApJ, 556, 515-532.

Pelletier,G. & Pudritz,R.E., 1992, ApJ, 394, 117.
bibitem Remillard, R.A. & McClintock, J.E., 2006, ARAA, 44, 49.

Rodriguez, J., Varnière, P., Tagger. M., and Durouchoux, P., 2002, A& A, 387, 487-496.

Sobczak, G.J., McClintock, J.E., Remillard, R.A., et al., 2000, ApJ, 531, 537.

Tagger, M., and Pellat, R., 1999, A&A, 349 1003, (TP99).

Tagger,M., Varnière,P., Rodriguez,J. & Pellat,R., 2004, ApJ, 607, 410-419.

Tomsick J.A., and Kaaret, P., 2001, ApJ, 548, 401

Trudolyubov, S., Churazov, E., Gilfanov, M., et al., 1999, A&A, 342, 496,

Varnière, P., Rodriguez, J. and Tagger. M., 2002, A&A, 387, 497-506.

Varnière, P. and Tagger. M., 2002, A&A, 394, 329-338.